Chemical Science

ROYAL SOCIETY OF CHEMISTRY

EDGE ARTICLE

View Article Online
View Journal | View Issue

Cite this: *Chem. Sci.*, 2025, **16**, 3916

All publication charges for this article have been paid for by the Royal Society of Chemistry

Total syntheses of cyclohelminthol I–IV reveal a new cysteine-selective covalent reactive group†

Thomas T. Paulsen, ‡[a] Anders E. Kiib, ‡[a] Gustav J. Wørmer,[a] Stephan M. Hacker [b] and Thomas B. Poulsen *[a]

Biocompatible covalent reactive groups (CRGs) play pivotal roles in several areas of chemical biology and the life sciences, including targeted covalent inhibitor design and preparation of advanced biologic drugs, such as antibody–drug conjugates. In this study, we present the discovery that the small, chlorinated polyketide natural product cyclohelminthiol II (**CHM-II**) acts as a new type of cysteine/thiol-targeting CRG incorporating both reversible and irreversible reactivity. We devise the first syntheses of four simple cyclohelminthols, (±)-cyclohelminthol I–IV, with selective chlorinations (at C_2 and C_5) and a Ni-catalyzed reductive cross coupling between an enone, a vinyl bromide and triethylsilyl chloride as the key steps. Unbiased biological profiling (cell painting) was used to discover a putative covalent mechanism for **CHM-II** in cells with subsequent validation experiments demonstrating mechanistic similarity to dimethyl fumarate (DMF) – a known (covalent) drug used in the treatment of multiple sclerosis. Focused biochemical experiments revealed divergent thiol-reactivity inherent to the **CHM-II** scaffold and through further chemical derivatization of **CHM-II** we applied activity-based protein profiling (ABPP)-workflows to show exclusive cysteine-labelling in cell lysate. Overall, this study provides both efficient synthetic access to the **CHM-II** chemotype – and neighboring chemical space – and proof-of-concept for several potential applications of this new privileged CRG-class within covalent chemical biology.

Received 23rd December 2024
Accepted 6th January 2025

DOI: 10.1039/d4sc08667h

rsc.li/chemical-science

Introduction

Covalent protein modification by synthetic ligands is re-emerging as a foundational area in the life sciences. This paradigm enables diverse applications and innovative technologies for chemical biology and drug discovery, ranging from precision *in vitro* protein functionalization,[1] *e.g.* to tune the properties of biologic drugs, to the discovery of new avenues for pharmacological modulation of previously untenable disease-mediating proteins.[2]

A vital component of any reagent for covalent protein modification is the electrophilic motif, also referred to as the covalent reactive group (CRG) or warhead,[3] that directly mediates binding to specific amino acid side chains. We, along with many others, have taken interest in continued innovation of CRG-chemistry due to the potential impact on a series of specific areas, including bioconjugation,[4–8] selective protein *in situ* labelling,[9,10] targeted covalent inhibitor design,[11,12] (re)-activity based protein profiling (ABPP) methods,[13–17] covalent PROTACs[18,19] and covalent fragments for screening.[20,21] Natural products have traditionally served as a rich source of inspiration for specific CRGs and how these can be embedded within – often complex – molecular scaffolds.[22–24] The penicillins (β-lactam CRG) and epoximicin (epoxide CRG) are classic examples with direct medical perspectives. Within this area, halogenated natural products occupy an inherently interesting position, due to the strong polarity of the carbon–halogen bond, which may directly confer covalent reactivity, or, alternatively, may tune the overall electronics of other types of reactive functionalities.

On this background, we became interested in the cyclohelminthols, which are a group of fungal polyketides, related to terrein,[25] produced by *Helminthosporium velutinum* yone96, a strain collected from a dead woody plant in Kagoshima, Japan. The Hashimoto group has been successful in isolating a number of secondary metabolites from the fungus with the first being cyclohelminthol I–IV reported in 2016 (Fig. 1, **1–4**).[26] These are the simplest members of their family, and they vary in the oxidation state at C_1 as well as by the number of chlorine atoms in the structure. In terms of known biological activity, cyclohelminthol II (**2**) was shown to be cytotoxic to human colon adenocarcinoma cells (COLO 201, IC_{50}: 58 μM) and human promyelocytic leukemia cells (HL60, IC_{50}: 11.5 μM), while the other three members showed only weak or no cytotoxicity in the

[a]*Department of Chemistry, Aarhus University, Langelandsgade 140, 8000 Aarhus C, Denmark. E-mail: thpou@chem.au.dk*

[b]*Leiden Institute of Chemistry, Leiden University, Einsteinweg 55, 2333 CC Leiden, The Netherlands*

† Electronic supplementary information (ESI) available. See DOI: https://doi.org/10.1039/d4sc08667h

‡ These authors contributed equally.

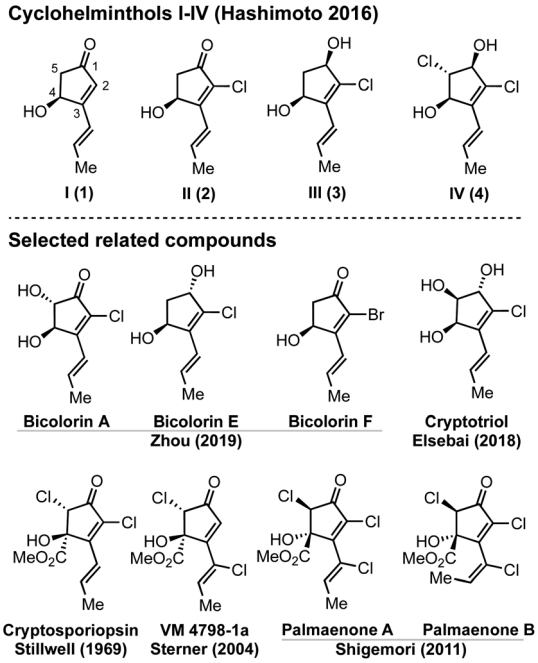

Fig. 1 Cyclohelminthol I–IV and related natural products. Name and year refer to isolation study.

same cell lines.[26] Albeit scarcely characterized, these initial studies indicate that the α-chloroenone motif may be particularly important for biological activity.

In addition to **1–4**, a series of structurally related halogenated fungal polyketides have also been reported. These include cryptotriol, which was shown to have broad-spectrum antibiotic activity[27] and the bicolorins, where congener A and F were found to have antifungal activity.[28] At a further level of structural complexity, cryptosporiopsin and related C_4-quaternary compounds, which display diverse activities, are also known.[29–31]

Despite the ubiquitous presence of potentially reactive sites in these compounds, and their apparent differing biological activity resulting from seemingly small changes in structure, no studies of their covalent reactivity have, to the best of our knowledge, been reported. Especially the simple members of the family appear interesting as they possess the size of the standard CRGs used in covalent chemical biology. In this paper, we report the first syntheses of cyclohelminthols I–IV and employ unbiased biological profiling experiments to discover the cellular activities of cyclohelminthol II (shortened **CHM-II**) to resemble those of dimethyl fumarate and sulforaphane, suggesting covalent reactivity. Detailed studies revealed that **CHM-II** indeed is a new class of CRG, which possesses unique, cysteine-focused reactivity, that may enable several different applications within covalent chemical biology.

Results and discussion

Syntheses of (±)-cyclohelminthol I–IV

The synthesis commenced from furfuryl alcohol (**5**), which was transformed into TBS protected alcohol **7** following the procedure of Curran *et al.*[32] in a yield of 28% over two steps (Scheme 1A). Following experimentation with various unsuccessful chlorination procedures (Scheme 1B), it was found that when **7** was treated with Mioskowski's reagent (Et_4NCl_3),[33] the enone was rapidly chlorinated. To ensure full elimination of the resulting dichloride to give the desired α-chloroenone **8**, it was necessary to treat the reaction mixture with Et_3N once full conversion of **7** was obtained. Following aqueous workup, **8** was obtained in near quantitative yield and further purification was unnecessary.

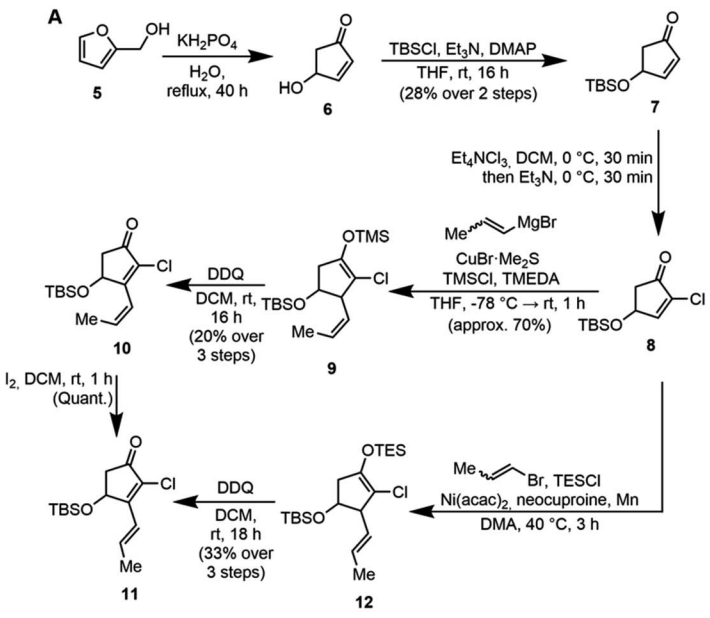

B

Entry	Failed chlorination conditions
1	PhSeCl, pyr, DCM, 40 °C, 21 h
2	PhSeCl, NCS, MeCN, rt, 24 h
3	*m*-CPBA, HCl·dioxane, rt, 30 min
4	Pyr·HCl, bisacetoxyiodobenzene, DCM, rt, 24 h

C

Entry	Conditions for oxidation of 9	10	S1
1	IBX, DMSO, rt, 1 h	10%	20%
2	IBX·MPO, DMSO, rt, 1 h	3%	15%
3	IBX·NMO, DMSO, rt, 1 h	5%	30%
4	$Pd(OAc)_2$, BQ, MeCN, rt, 24 h	0%	60%
5	$Pd(OAc)_2$, DMSO, O_2, rt, 2.5 h	0%	40%
6	$Pd(OAc)_2$, AMC, MeCN, reflux, 22 h	0%	50%
7	DDQ, DCM, rt, 16 h	30%	30%
8	DDQ, benzene, rt, 16 h	15%	45%
9	DDQ, MeCN, rt, 16 h	15%	55%
10	DDQ, 2,4,6-collidine, DCM, rt, 16 h	10%	40%
11	DDQ, HMDS, rt, 16 h	10%	60%
12	DDQ, BSA, rt, 16 h	3%	60%

Yields are only for the oxidation reaction and are based on 70% in the conjugate addition.
BQ = benzoquinone; AMC = allyl methyl carbonate

Scheme 1 (A) Preparation of intermediate **11** common for (±)-cyclohelminthol II–IV, (B) failed conditions for the chlorination of **7** and (C) optimization of the oxidation of **9**.

Our initial approach for introduction of the (*E*)-propenyl sidechain was conjugate addition to chloroenone **8** with trapping of the resulting enolate as a silyl enol ether.[34] In turn, the silyl enol ether would be oxidized to afford the corresponding α,β,γ,δ-unsaturated ketone. While the conjugate addition of 1-propenylmagnesium bromide proceeded well (70% yield by ^{1}H NMR), all oxidation conditions attempted led to a significant amount of hydrolysis product **S1** (Scheme 1C). The most promising was oxidation using DDQ (DCM, rt, 16 h) which gave the desired enone **10** in 30% yield along with 30% of **S1**. This sequence could be carried out in 20% overall yield from **7** without purification of **8** or **9**. Interestingly, the conjugate addition led exclusively to the undesired (*Z*)-configuration of the olefin, however, following the oxidation, equilibration to the desired (*E*)-configuration (compound **11**) could be performed in quantitative yield by treatment with catalytic iodine. The strong tendency of compound **9** for hydrolysis indicated that a more stable silyl enol ether could be beneficial, however, attempts at conducting the conjugate addition using TESCl, TESOTf, TBSCl and TBSOTf did not yield the desired silyl enol ethers even at elevated temperatures, possibly due to the activating role of TMSCl in the conjugate addition.[35,36] It was ultimately found that a reductive cross coupling, as reported by Weix and coworkers, provided a convenient alternative.[37] Despite only a single vinyl bromide being included in the original substrate scope, we found that 1-bromopropene (purchased as a mixture of (*E*)/(*Z*)-isomers) reacted with chloroenone **8** and triethylsilyl chloride to give the desired silyl enol ether **12**. While the copper-catalyzed conjugate addition delivered the (*Z*)-isomer, this reductive cross coupling gave predominantly (>19 : 1) the desired (*E*)-configuration of the propenyl group, meaning that the iodine isomerization was unnecessary. Following column chromatography on silica gel, TES enol ether **12** was isolated in 55% yield. Oxidation of **12** using DDQ led to formation of the desired enone **11** in 59% yield after column chromatography. More conveniently, the oxidation was carried out without purification of **12**, yielding the α,β,γ,δ-unsaturated ketone **11** in 33% yield over three steps from **7**.

Using the same reductive cross coupling and DDQ oxidation sequence from **7**, TBS-protected (±)-cyclohelminthol I (**13**) could be obtained with yields of 65% and 54% respectively as seen in Scheme 2A. Deprotection of the secondary alcohol was achieved using TBAF buffered with acetic acid, delivering (±)-cyclohelminthol I (**1**) in 70% yield. Likewise, deprotection of chloroenone **11** would give (±)-cyclohelminthol II (**2**) but surprisingly, treatment with TBAF led only to decomposition of the starting material. Following screening of conditions, it was found that treatment of **11** with *in situ* generated HCl in methanol gave clean deprotection yielding (±)-cyclohelminthol II (**CHM-II**, **2**) in 81% yield (Scheme 2B).

To gain access to (±)-cyclohelminthol III, the ketone of **11** would have to be reduced in a diastereoselective fashion. Reduction under Luche conditions led to a mixture of

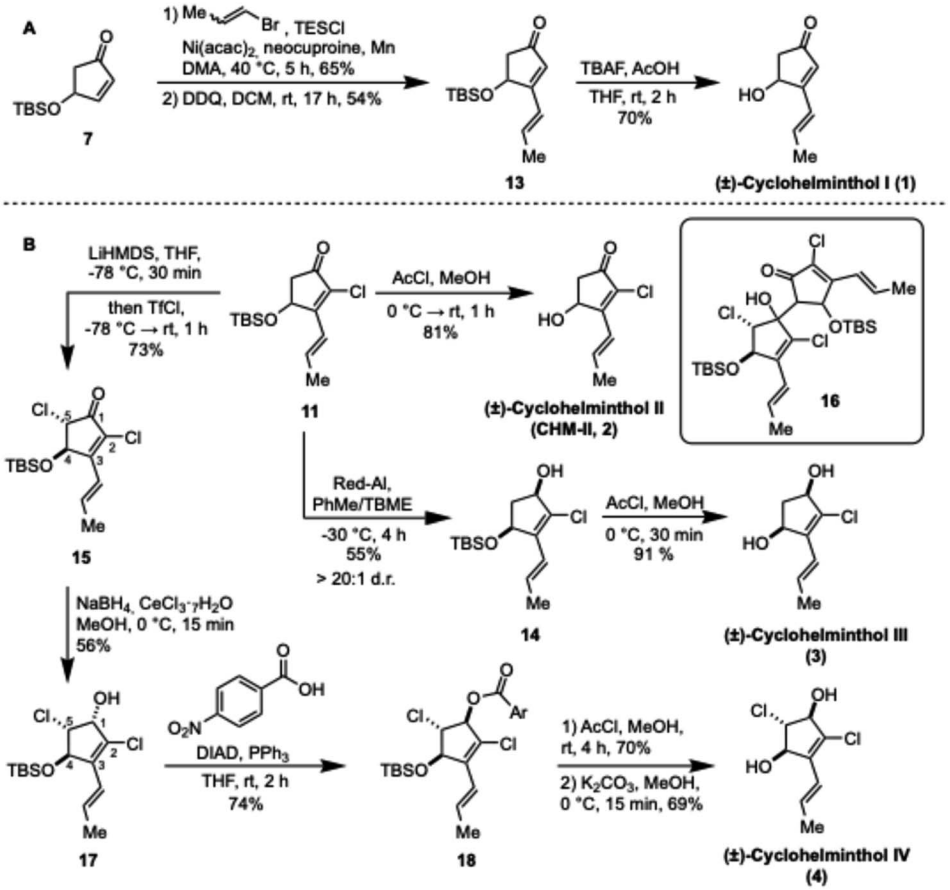

Scheme 2 Completion of syntheses of (A) (±)-cyclohelminthol I and (B) (±)-cyclohelminthol II–IV.

diastereoisomers (2 : 1 *cis*/*trans*, total yield 66%). Satisfyingly, reduction with Red-Al at −30 °C selectively afforded the desired stereoisomer **14** in 55% yield (>20 : 1 d.r.).[32] The obtained *cis*-alcohol **14** could be deprotected using HCl in MeOH yielding (±)-cyclohelminthol III (**3**) in 91% yield.

Having secured access to cyclohelminthol I–III, we finally pursued cyclohelminthol IV. Towards that end, we first attempted α-chlorination of **11** under acidic conditions (thionyl chloride or NCS/TsOH), but no reactivity was observed. Switching instead to basic conditions, deprotonation using LiHMDS, followed by treatment with NCS led to clean monochlorination, yielding the desired α-chloroenone **15** in 70% yield on small scale (10 mg of **11**).[38] However, when this reaction was attempted at a slightly larger scale (100 mg of **11**) the yield dropped to 40% and, interestingly, a significant amount of dimer **16** – resulting from aldol reaction of the enolate from **11** and the generated **15** – was isolated. Exchanging the chlorinating reagent for the more reactive trifluoromethanesulfonyl chloride, however, resolved the problem of dimer formation[39] and the desired product **15** could be isolated in 73% yield (scale: 220 mg of **11**).

Reduction of α-chloroenone **15** was investigated with several different reducing agents, with the best result being obtained using Luche conditions, which yielded the alcohol **17** as a single diastereoisomer in 56% yield. However, upon deprotection it was clear that **17** was the undesired 1,5-*cis*-4,5-*trans*-isomer, as the resulting diol (**S4** in ESI†) did not match cyclohelminthol IV for which the crystal structure has been solved leaving no ambiguity of its configuration.[26] The diastereoisomer **17** was formed exclusively, even with bulky reducing agents such as DIBAL-H, suggesting that the diastereoselectivity of ketone reduction is controlled by the chloride substituent and, surprisingly, not the OTBS group. Fortunately, inversion of the newly generated stereocenter could be achieved through a Mitsunobu strategy, where **17** was first treated with 4-nitrobenzoic acid, diisopropyl azodicarboxylate (DIAD) and triphenylphosphine in THF, to obtain ester **18** in 74% yield. Deprotection of the silyl ether with HCl in methanol proceeded in 70% yield and was followed by cleavage of the 4-nitrobenzoate group in basic methanol to yield (±)-cyclohelminthol IV (**4**) in 69% yield. This thereby completed the first total syntheses of (±)-cyclohelminthol I–IV. The spectroscopic data of all four natural products match those reported with their isolation.[26]

Unbiased morphological profiling identifies cyclohelminthol II as a putative covalent modifier

To gain insights into the biological activities of **1–4**, we initially investigated their cytotoxicity in a panel of human cell lines

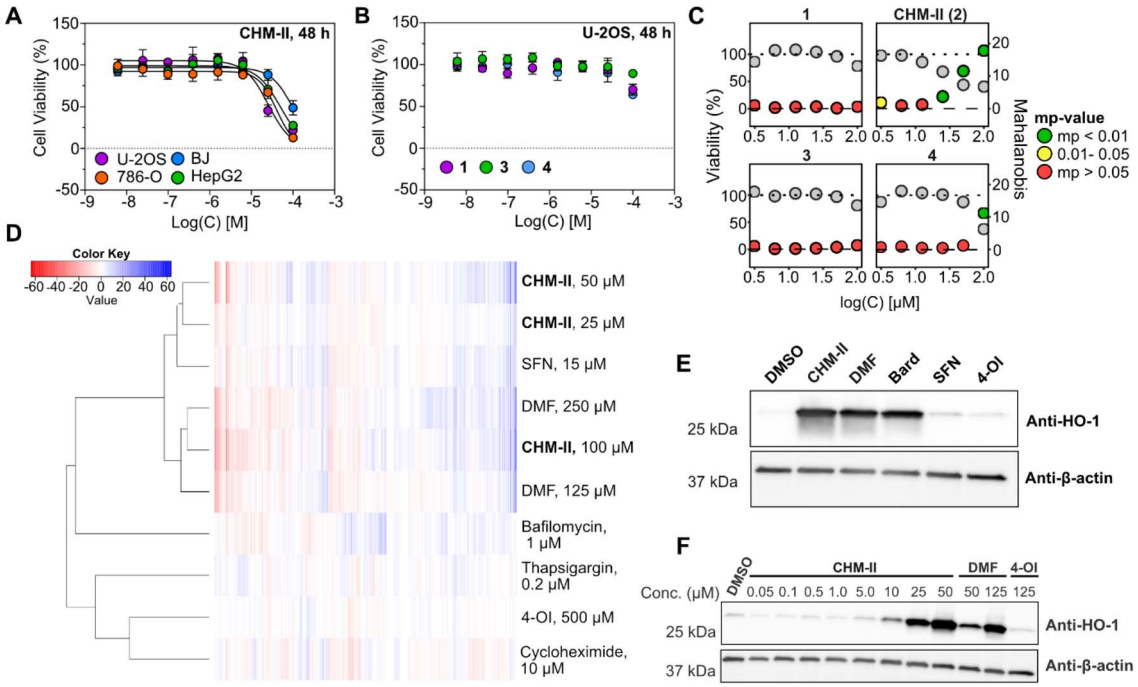

Fig. 2 The cellular activities of cyclohelminthol II (**CHM-II**, **2**) resemble those of dimethyl fumarate. (A) Representative cell viability curves after 48 hours of treatment with **CHM-II** in four different cell lines. Data points are mean ± sd ($N = 3$) and curves were fitted through 4-parameter nonlinear regression in GraphPad Prism 10.2.3. IC_{50}-values (see text) are means of three biological replicates (four for the BJ cell line). (B) Representative viability plot after 48 hours of treatment of U-2OS cells with **1**, **3**, or **4**. (C) Dose–response curves of cell viability (left axis) and activity score as represented by the Mahalanobis distance (right *y*-axis) and the mp-value from the cell painting assay. Concentrations for which the mp-value <0.01 (multiple perturbation value) were considered active. (D) Heatmap of morphological profiles showing strong similarity between **CHM-II** and the covalent modifiers dimethyl fumarate (DMF) and sulforaphane (SFN) in U-2OS cells. Clustering was performed by hierarchical clustering and compound treatment duration was 24 hours. (E) Representative western blot utilizing a heme oxygenase 1 (HO-1) specific antibody after 21 hours of treatment with various HO-1 inducers in U-2OS cells. **CHM-II** (**2**) (50 μM): cyclohelminthol II, DMF (125 μM): dimethyl fumarate, Bard (500 nM): bardoxolone methyl ester, SFN (15 μM): sulforaphane, 4-OI (125 μM): 4-octyl itaconate. β-Actin was used as loading control. (F) Dose–response of the HO-1 induction after 24 hours of treatment in U-2OS cells with western blotting as readout.

containing osteosarcoma (U-2OS), renal carcinoma (786-O), hepatoblastoma (HepG2), and non-cancerous fibroblast cells (BJ). In accordance with reports from the isolation studies,[26] we found cyclohelminthol II (**CHM-II**, **2**) to be the only compound displaying any noteworthy cytotoxicity. Interestingly, highest activity was observed in the U-2OS cell line (IC_{50}: 24.3 μM ± 3.9 μM), followed by the 786-O (IC_{50}: 41.8 μM ± 3.9 μM) and HepG2 (IC_{50}: 46.9 μM ± 10.7 μM) cell lines. In comparison, the non-cancerous BJ cell line (IC_{50}: 93.6 μM ± 13.1 μM) displayed a slightly increased tolerance towards **CHM-II**. To obtain a much broader coverage of the compounds' cellular activities, we next employed morphological profiling *via* cell painting (CP). CP is an image-based, high-throughput bioactivity-profiling method, developed by the Carpenter lab,[40] that can detect compound-induced cellular perturbations through morphological alterations to the cellular ultrastructure as visualized by fluorescence microscopy.[41] Several recent studies have demonstrated that CP is a highly sensitive method for detecting biological activity *per se*,[42,43] which can be employed to generate (broad) mechanistic hypotheses of novel compounds through statistical correlations of their bioactivity fingerprints to that of mechanistically-annotated reference compounds.[40,42,44,45] We employed our optimized CP-workflow[41] in U-2OS osteosarcoma cells and evaluated **1–4** in a range of different doses.

In accordance with the cytotoxicity studies, only **CHM-II** (**2**) displayed significant activity in the CP assay (defined as mp-value <0.01. The mp-value is a multiple perturbation value described by Hutz *et al.* as a measure of statistical significance in multivariate data)[42,46] at concentrations below 100 μM (from 25 μM, Fig. 2C). Upon subsequent comparison of the morphological profiles with our in-house profile library – containing profiles of 532 compounds at multiple concentrations – **CHM-II** (**2**) was found to correlate strongly (Pearson coefficient > 0.7, Fig. S1†) to sulforaphane (SFN) and dimethyl fumarate (DMF), two covalently acting compounds[47,48] of which the latter has been used in the treatment of multiple sclerosis since 2013 (Tecfidera®).[49] Interestingly, the profiles were found to further sub-cluster with the highest concentration of **CHM-II** correlating more strongly with DMF, while the profiles obtained at lower concentration have slightly higher correlations with SFN (Fig. 2D and S2†). DMF and SFN are well-known to have multiple (covalent) biological targets through cysteine-alkylation,[47,48] and the observed correlations strongly suggest that **CHM-II** also acts through a covalent mechanism.

As DMF and SFN are both known inducers of heme oxygenase 1 (HO-1, HMOX1), albeit to very different extent,[50,51] we subsequently investigated if **CHM-II** (**2**) shared this activity through western-blotting experiments with a HO-1-specific antibody. Indeed, **CHM-II** was found to induce HO-1 to similar levels as DMF when used at less than half the concentration (50 μM *vs.* 125 μM) and significant induction was observed already at 10 μM **CHM-II**. In comparison, HO-1 induction by **CHM-II** was significantly higher than with SFN and 4-octyl itaconate (4-OI) (Fig. 2E, F and S3†). 4-OI has multiple immunomodulatory effects and is a KEAP1 binder and NRF2-activator[52] which is known to induce HO-1 expression in several cell lines, such as 786-O cells (Fig. S4†). The lack of notable HO-1 induction observed for 4-OI in U-2OS cells – in the light of the strong HO-1 induction triggered by **CHM-II** – suggest that **CHM-II**, interestingly, is acting through a different mechanism than 4-OI. While HO-1 has been linked to several therapeutically relevant mechanisms in recent years much still remains unknown.[53] Therefore, new modalities and tools modulating HO-1 expression remain of interest from both a basic science and a therapeutic point of view.

Cyclohelminthol II reacts both reversibly and irreversibly with thiol nucleophiles

With these insights from the CP-experiments, we next studied the reactivity of **CHM-II** (**2**) towards thiols under preparative conditions and in aqueous buffers. For these experiments, we employed methyl thioglycolate (MTG) as a model thiol. Under preparative conditions using 3 equivalents of MTG and 2 equivalents of 1,8-diazabicyclo[5.4.0]undec-7-ene (DBU) in dichloromethane, we could isolate the 1,6-addition product **19** (41%), and, surprisingly, the double addition adduct **20** (40%) where another equivalent of MTG had substituted the chloride at C_2 (Fig. 3A). We next studied the properties and reactivity of **CHM-II** (**2**) in aqueous buffers (Fig. 3B and C). The compound was stable for at least 21 h under aqueous conditions (phosphate buffer, pH 8.1, 10% MeCN), but converted rapidly in the presence of MTG to afford **19** and a very minor amount of **20** (Fig. 3B, C and S6–S8.† A half-life of 46.6 minutes was determined through fitting to a one-phase decay function). Interestingly, an unknown compound (**21**, R_t = 3.54 min) was also formed in these experiments which, by LC-MS/MS-analysis, matched a product corresponding to direct substitution of the α-chloride of **CHM-II** (**2**) by the thiol (Fig. S9†). While compounds **19** and **20** clearly proved stable to purification under preparative conditions, thio-Michael additions are well-known to be reversible depending on the conditions.[54,55] We therefore studied the behavior of purified **19** and **20** in aqueous buffers and indeed observed that **19** reverted back to **CHM-II** (**2**) whereas **20** generated the aforementioned compound **21** (Fig. S10 and S11†). Performing this last reaction under preparative conditions allowed the unambiguous assignment of the structure of **21** (Fig. 3D and S12†). Mechanistically, this rather surprising spectrum of reactivity of **CHM-II** (**2**) might be rationalized as illustrated in Fig. 3E: following initial, reversible, 1,6-addition, an additional thiolate could reversibly add to the β-carbon of the enone to afford an α-chloroketone intermediate (**INT-1**). This compound is activated towards irreversible displacement of the chloride by a third thiolate forming **INT-2** and subsequent β-elimination then affords the observed compound **20**. An alternative possibility involves the formation of a thiiranium ion (**INT-3**) by expulsion of the chloride by the proximal sulfide formed from 1,4-addition, again followed by β-elimination. From **20**, compound **21** can be formed by final thiol-elimination (Fig. 3E). Overall, these *in vitro* experiments demonstrate that **CHM-II** (**2**) possesses biologically relevant reactivity towards thiols, including both reversible 1,6-addition and, irreversible substitution of the α-chloride.

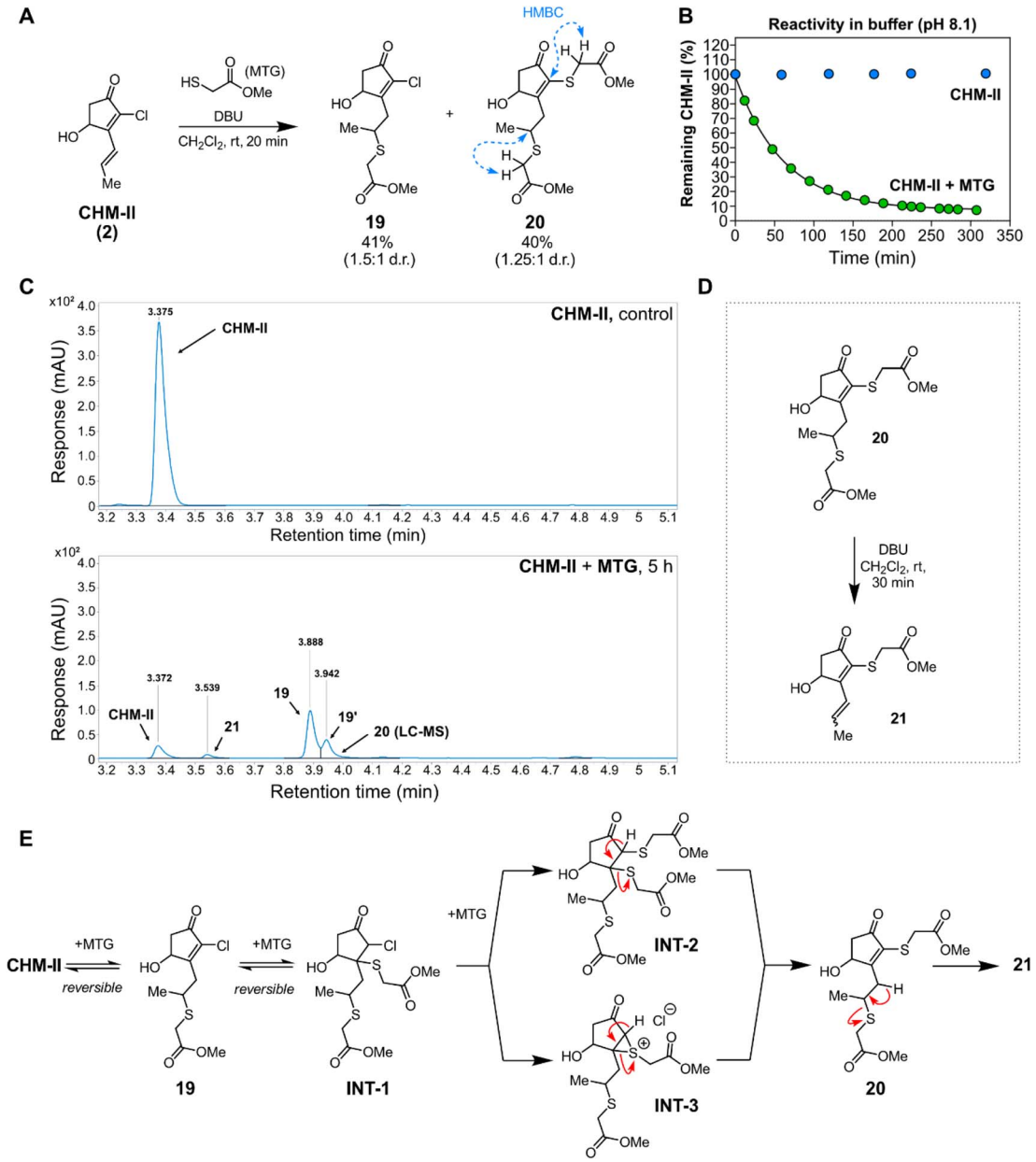

Fig. 3 Examination of the thiol reactivity of **CHM-II** (**2**) under preparative conditions and in aqueous buffers. (A) Preparative synthesis of mono- and diconjugated species **19** and **20** (mixture of diastereomers) through reaction of **CHM-II** (**2**) with methyl thioglycolate (MTG). (B) Stability of **CHM-II** in aqueous phosphate buffer (pH 8.1, 10% MeCN) with and without the presence of MTG (1 mM). The half-life of **CHM-II** in the presence of MTG, 46.6 minutes, was determined through fitting to a one-phase decay function in GraphPad Prism version 10.2.3 for Windows. (C) HPLC chromatograms of the control sample of **CHM-II** in phosphate buffer (top) and the reaction mixture containing both **CHM-II** and MTG after 5 hours (bottom) at 260 nm. **19** and **19′** refer to the two diastereomers of the 1,6-addition product. Full chromatograms in ESI.† Note that **CHM-II** and the conjugation products display notably different UV-absorbance (Fig. S13†). (D) Reaction scheme for the preparative synthesis of compound **21**. (E) Potential mechanisms for formation of compounds **19**–**21**.

Functionalized cyclohelminthol II derivatives as covalent probes

We also investigated derivatization of **CHM-II** to unlock potential broader application as a covalent handle/probe. While several different functionalization strategies of **CHM-II** can be envisioned, we were particularly interested in modification at the C_4-hydroxyl group as this provides a minimal perturbation of the overall structure of the reactive functional group(s). Towards this end, we found that alkylation of the C_4-hydroxyl could be performed using trichloroacetimidates[56] (see ESI†) allowing *e.g.* for the preparation of the 'minimal' alkyne-tagged derivative **CHM-II-alk** (**22**) (Fig. 4A). **CHM-II-alk** was found to induce expression of HO-1 to similar levels as **CHM-II** in U-2OS cells (Fig. S14†), indicating that the modification on the C4-hydroxyl was tolerated without apparent loss of biological activity. Alternatively, the C_4-hydroxyl group can also be

functionalized *via* an isocyanate-PFP-ester glycine unit to form an intermediate carbamate-linked PFP-ester **S6** (see ESI, Fig. S15†). The PFP-ester then enables smooth amide bond formation using *e.g.* an exemplary amine equipped with both a diazirine and an alkyne to afford **S7** in high yield. This example showcases that **CHM-II** can be introduced as a new CRG through standard amide formation (Fig. S15†).

To directly explore whether the covalent reactivity observed in the preparative and buffer-based settings was translatable to biological systems, we next incubated U-2OS cells overnight with varying concentrations of **CHM-II-alk** (22). By subsequently employing a gel-based ABPP workflow involving conjugation of **CHM-II-alk**-bound proteins to a fluorophore (5-TAMRA-azide) *via* copper-catalyzed azide–alkyne cycloaddition (CuAAC) and separation of the proteins by SDS-PAGE, we were able to visualize covalent targets of **CHM-II-alk** in the U-2OS proteome (Fig. 4B). Indeed, concentration-dependent labelling of several proteins were observed in live U-2OS cells (Fig. 4C) as well as in lysate (Fig. S16†), which, considering the harsh conditions of the SDS-PAGE (boiling in denaturing and reducing conditions), confirmed the ability of **CHM-II-alk** to form stable, non-reversible covalent bonds with proteins under biological conditions. This further highlights the potential use of **CHM-II** and its derivatives as a CRG.

Based on the thiol-reactivity observed in buffer and under preparative conditions, we hypothesized that the covalent reactivity observed in live cells and lysate was primarily cysteine-mediated. To test this hypothesis, we initially conducted a competitive gel-based ABPP experiment, in which U-2OS lysate samples were pre-treated with iodoacetamide (IA), a well-established broadly cysteine-reactive reagent, at various concentrations prior to treatment with **CHM-II-alk**. In accordance with our hypothesis, IA pre-treatment effectively abated labelling by **CHM-II-alk** in a concentration-dependent manner (Fig. 4D), strongly suggesting that the main reactivity of **CHM-II-alk** is, indeed, cysteine-oriented. To further confirm the

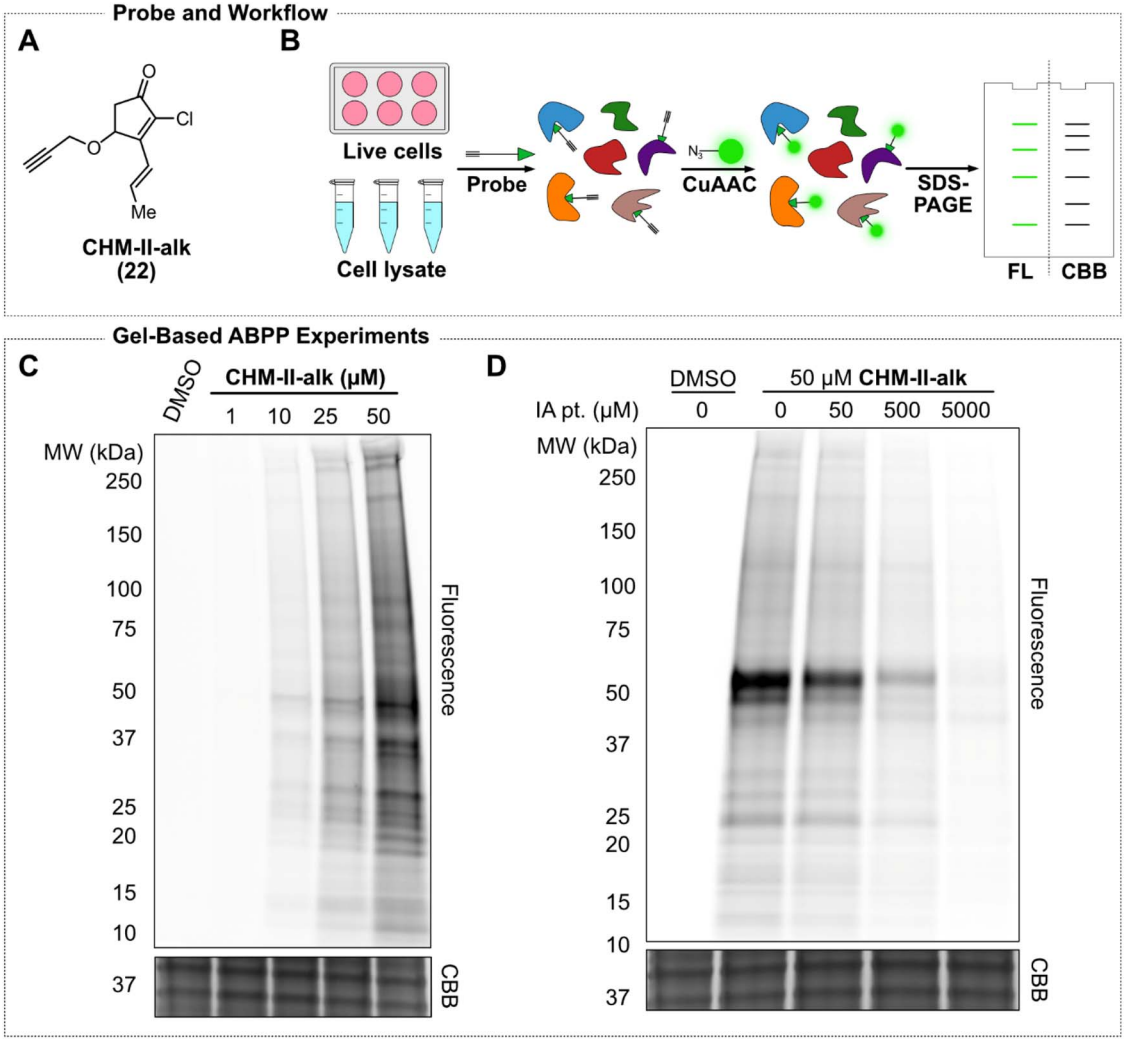

Fig. 4 Gel-based profiling of the protein targets of an alkyne-tagged cyclohelminthol II derivative. (A) The structure of alkyne-tagged derivative of cyclohelminthol II (**CHM-II-alk**, **22**). (B) Graphical representation of the gel-based ABPP workflow. (C) In-gel fluorescence observed following overnight (18 h) treatment of U-2OS cells with **CHM-II-alk**. (D) Competitive protein profiling in U-2OS cell lysate. Samples were pre-treated with iodoacetamide (IA) at varying concentrations for one hour (IA pt.), followed by treatment with 50 μM **CHM-II-alk** for two hours. ABPP: activity-based protein profiling, FL: fluorescence, CBB: Coomassie brilliant blue (general protein stain).

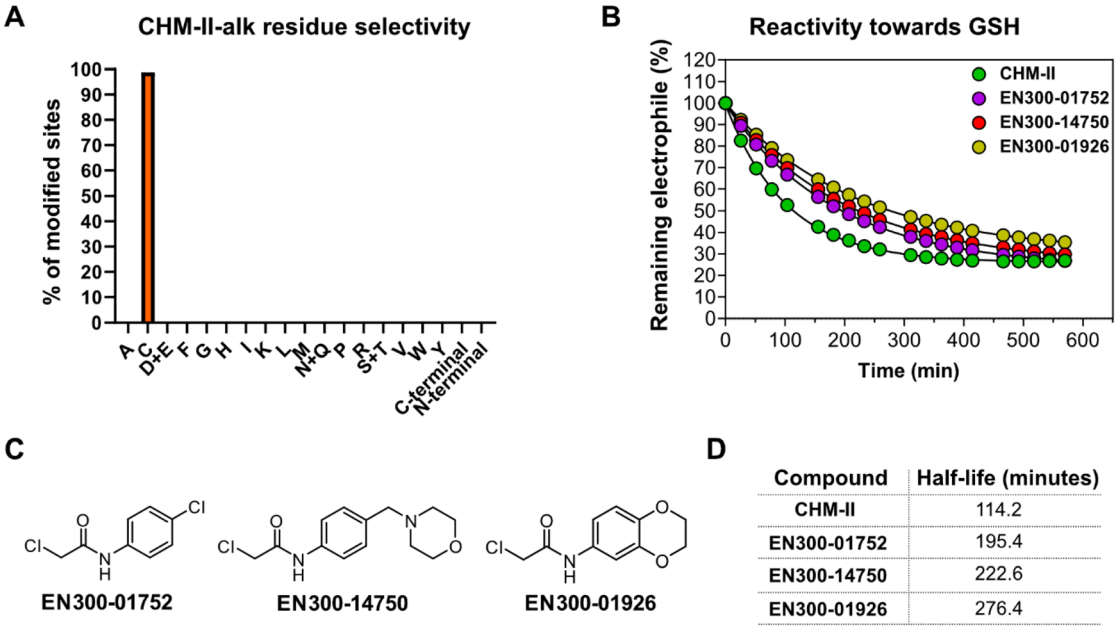

Compound	Half-life (minutes)
CHM-II	114.2
EN300-01752	195.4
EN300-14750	222.6
EN300-01926	276.4

Fig. 5 Residue selectivity of **CHM-II-alk** and HPLC-based GSH reactivity assay. (A) Residue selectivity (98.8%) observed for **CHM-II-alk** based on 248 modification sites observed in three of four samples. (B) Compound (200 μM) reactivity towards reduced GSH (1 mM) in potassium phosphate buffer (100 mM, pH 8.1) containing 10% MeCN, as measured by the reduction of the compound peak integrals (at 260 nM) over time. Half-lives were determined through fitting to a one-phase decay equation in GraphPad Prism version 10.2.3 for Windows. (C) Structures of the investigated chloroacetamide containing compounds. The names correspond to the catalogue IDs in the Enamine store, https://new.enaminestore.com/. (D) The half-lives determined in the HPLC-based GSH reactivity assay. GSH: glutathione.

apparent cysteine selectivity, we next utilized **CHM-II-alk** in the unbiased, proteome-wide amino acid selectivity chemoproteomics workflow developed by Zanon *et al.*[17] (workflow in ESI†), which relies on open- and offset-search analyses using the MSFagger-based FragPipe computational platform.[57–62] Interestingly, while the main modification observed in the open-search analysis was found to match the mass expected for mono-addition without the loss of Cl, significant loss of Cl was also observed (Fig. S17†), suggesting that both types of conjugation products might hold biological relevance. Using the main observed modification masses for the subsequent offset-search analysis, **CHM-II-alk** was found to be 98.8% cysteine selective (based on 248 modification sites observed in three out of four samples, Fig. 5A), while 1121 cysteine residues from 733 proteins could be quantified in a closed search analysis (Fig. S18†).

It should be noted that while the selectivity experiment does yield a list of protein targets obtained through the closed search (available on OSF), the experimental setup does not allow for determination of the degree of modification or target affinity, and as such care should be taken when drawing conclusions based on the observed targets – especially since the experiment was conducted in cell lysate using 300 μM **CHM-II-alk**.

With the apparent cysteine reactivity in mind, we next sought to obtain quantitative information of the reactivity of **CHM-II** compared to other known thiol-targeting compounds using two different approaches. Specifically, we first employed the reactivity assay reported by Resnick and co-workers involving reduced Ellman's reagent (5-dithio-bis-2-nitrobenzoic acid, DTNB) (Fig. S19†)[63] but found that the reactivity of **CHM-II** was below the minimal threshold detected by this specific assay. However, as the DTNB-based assay may underestimate the reactivity of α,β-unsaturated carbonyl systems we therefore sought to compare the glutathione (GSH) reactivity of **CHM-II** to that of three chloroacetamide-containing covalent fragments (Fig. 5C) in an HPLC-based experiment. Through incubation of each compound (200 μM) with reduced GSH (1 mM) in aqueous buffer solution (potassium phosphate containing 10% MeCN, pH 8.1), half-lives were determined as a relative measure of reactivity (Fig. 5B, D, and S12–S23†). Based on the observed half-lives, it is clear that the DTNB-based assay did indeed underestimate the reactivity of **CHM-II**, which the HPLC-based assay showed to be comparable to the investigated chloroacetamides. Although chloroacetamides are usually considered among the more reactive cysteine reactive groups used in covalent inhibitors, their reactivity has been shown to be well-suited for covalent fragment-based drug discovery (FBDD).[63,64] Taken together, these data support that **CHM-II**, being a natural product and thus a privileged scaffold, represents a novel cysteine-targeted CRG in the chemical biology toolbox.

Conclusions

In this study, we have identified the natural product cyclohelminthol II (**CHM-II**, **2**) as a new type of covalent reactive group (CRG) which we believe enables a series of different applications within chemical biology. In addition to providing access to **CHM-II** (**2**), our synthesis also allowed for the first preparation of cyclohelminthol I, III, and IV and the overall strategy is flexible and can likely support further exploration of

the chemical space around **1–4** in the future. We also demonstrate how **CHM-II** can be functionalized to enable appendage to other building blocks *via* CuAAC or amide couplings. We employed several different experiments to first identify and then study in detail the covalent reactivity of **CHM-II**. Interestingly, **CHM-II** was found to undergo divergent reactions with thiols, including both reversible (1,6-addition) and irreversible (formal α-chloride-substitution) conjugations as well as potentially addition to proximal bis-thiol sites. The gel-based and chemoproteomic ABPP experiments further support the observation that **CHM-II** can irreversibly ligand cysteine-sites within the proteome and future experiments will explore these targets in high detail. Prompted by the strong mechanistic correlation between **CHM-II** and DMF identified by the CP assay, further exploration of the potential immunomodulatory activities of **CHM-II** in relevant cellular models is also of interest.

Data availability

The data that support the findings of this study are available in the ESI† of this article. Raw data, including .gel files of gels and membranes, relevant scripts for data analysis, and NMR files are available at OSF (**https://doi.org/10.17605/OSF.IO/FEHN5**).

Author contributions

T. T. P. and G. W. performed organic synthesis. A. E. K. performed biochemical and cell biological studies. S. M. H. supervised the chemoproteomics experiments. T. B. P. supervised the project. T. T. P., A. E. K. and T. B. P. wrote the paper.

Conflicts of interest

The authors declare no conflicts of interest.

Acknowledgements

Financial support from Independent Research Fund Denmark (grant 2032-00219B), Novo Nordisk Foundation (grant NNF19OC0054782 and NNF23OC0086068) is acknowledged. This project has received funding from the European Research Council (ERC) under the European Union's Horizon 2020 research and innovation programme (grant agreement No. 865738). The aliquot of heme oxygenase 1 (HO-1) specific antibody used in this project was a kind gift from associate professor David Olagnier from the Department of Biomedicine at Aarhus University.

References

1 E. A. Hoyt, P. M. S. D. Cal, B. L. Oliveira and G. J. L. Bernardes, Contemporary Approaches to Site-Selective Protein Modification, *Nat. Rev. Chem.*, 2019, **3**(3), 147–171, DOI: **10.1038/s41570-019-0079-1**.

2 J. N. Spradlin, E. Zhang and D. K. Nomura, Reimagining Druggability Using Chemoproteomic Platforms, *Acc. Chem. Res.*, 2021, **54**(7), 1801–1813, DOI: **10.1021/acs.accounts.1c00065**.

3 L. Hillebrand, X. J. Liang, R. A. M. Serafim and M. Gehringer, Emerging and Re-Emerging Warheads for Targeted Covalent Inhibitors: An Update, *J. Med. Chem.*, 2024, **67**(10), 7668–7758, DOI: **10.1021/acs.jmedchem.3c01825**.

4 M. Nisavic, G. J. Wørmer, C. S. Nielsen, S. M. Jeppesen, J. Palmfeldt and T. B. Poulsen, oxSTEF Reagents Are Tunable and Versatile Electrophiles for Selective Disulfide-Rebridging of Native Proteins, *Bioconjugate Chem.*, 2023, **34**(6), 994–1003, DOI: **10.1021/acs.bioconjchem.3c00005**.

5 S. J. Walsh, S. Omarjee, W. R. J. D. Galloway, T. T.-L. Kwan, H. F. Sore, J. S. Parker, M. Hyvönen, J. S. Carroll and D. R. Spring, A General Approach for the Site-Selective Modification of Native Proteins, Enabling the Generation of Stable and Functional Antibody–Drug Conjugates, *Chem. Sci.*, 2019, **10**(3), 694–700, DOI: **10.1039/C8SC04645J**.

6 H. Faustino, M. J. S. A. Silva, L. F. Veiros, G. J. L. Bernardes and P. M. P. Gois, Iminoboronates Are Efficient Intermediates for Selective, Rapid and Reversible N-Terminal Cysteine Functionalisation, *Chem. Sci.*, 2016, **7**(8), 5052–5058, DOI: **10.1039/C6SC01520D**.

7 M. J. Matos, B. L. Oliveira, N. Martínez-Sáez, A. Guerreiro, P. M. S. D. Cal, J. Bertoldo, M. Maneiro, E. Perkins, J. Howard, M. J. Deery, J. M. Chalker, F. Corzana, G. Jiménez-Osés and G. J. L. Bernardes, Chemo- and Regioselective Lysine Modification on Native Proteins, *J. Am. Chem. Soc.*, 2018, **140**(11), 4004–4017, DOI: **10.1021/jacs.7b12874**.

8 C. E. Stieger, Y. Park, M. A. R. De Geus, D. Kim, C. Huhn, J. S. Slenczka, P. Ochtrop, J. M. Müchler, R. D. Süssmuth, J. Broichhagen, M. Baik and C. P. R. Hackenberger, DFT-Guided Discovery of Ethynyl-Triazolyl-Phosphinates as Modular Electrophiles for Chemoselective Cysteine Bioconjugation and Profiling, *Angew. Chem., Int. Ed.*, 2022, **61**(41), e202205348, DOI: **10.1002/anie.202205348**.

9 T. Tamura, T. Ueda, T. Goto, T. Tsukidate, Y. Shapira, Y. Nishikawa, A. Fujisawa and I. Hamachi, Rapid Labelling and Covalent Inhibition of Intracellular Native Proteins Using Ligand-Directed N-Acyl-N-Alkyl Sulfonamide, *Nat. Commun.*, 2018, **9**(1), 1870, DOI: **10.1038/s41467-018-04343-0**.

10 R. N. Reddi, A. Rogel, R. Gabizon, D. G. Rawale, B. Harish, S. Marom, B. Tivon, Y. S. Arbel, N. Gurwicz, R. Oren, K. David, J. Liu, S. Duberstein, M. Itkin, S. Malitsky, H. Barr, B.-Z. Katz, Y. Herishanu, I. Shachar, Z. Shulman and N. London, Sulfamate Acetamides as Self-Immolative Electrophiles for Covalent Ligand-Directed Release Chemistry, *J. Am. Chem. Soc.*, 2023, **145**(6), 3346–3360, DOI: **10.1021/jacs.2c08853**.

11 Y. Liu, Z. Yu, P. Li, T. Yang, K. Ding, Z.-M. Zhang, Y. Tan and Z. Li, Proteome-Wide Ligand and Target Discovery by Using Strain-Enabled Cyclopropane Electrophiles, *J. Am. Chem. Soc.*, 2024, **146**(30), 20823–20836, DOI: **10.1021/jacs.4c04695**.

12 J. K. Eaton, L. Furst, L. L. Cai, V. S. Viswanathan and S. L. Schreiber, Structure–Activity Relationships of GPX4

Inhibitor Warheads, *Bioorg. Med. Chem. Lett.*, 2020, **30**(23), 127538, DOI: **10.1016/j.bmcl.2020.127538**.

13 B. K. Hansen, C. J. Loveridge, S. Thyssen, G. J. Wørmer, A. D. Nielsen, J. Palmfeldt, M. Johannsen and T. B. Poulsen, STEFs: Activated Vinylogous Protein-Reactive Electrophiles, *Angew. Chem., Int. Ed.*, 2019, **58**(11), 3533–3537, DOI: **10.1002/anie.201814073**.

14 A. Mahía, A. E. Kiib, M. Nisavic, E. B. Svenningsen, J. Palmfeldt and T. B. Poulsen, α-Lactam Electrophiles for Covalent Chemical Biology, *Angew. Chem., Int. Ed.*, 2023, **62**(26), e202304142, DOI: **10.1002/anie.202304142**.

15 G. J. Wørmer, B. K. Hansen, J. Palmfeldt and T. B. Poulsen, A Cyclopropene Electrophile That Targets Glutathione S-Transferase Omega-1 in Cells, *Angew. Chem., Int. Ed.*, 2019, **58**(34), 11918–11922, DOI: **10.1002/anie.201907520**.

16 N. Ma, J. Hu, Z.-M. Zhang, W. Liu, M. Huang, Y. Fan, X. Yin, J. Wang, K. Ding, W. Ye and Z. Li, 2 *H* -Azirine-Based Reagents for Chemoselective Bioconjugation at Carboxyl Residues Inside Live Cells, *J. Am. Chem. Soc.*, 2020, **142**(13), 6051–6059, DOI: **10.1021/jacs.9b12116**.

17 P. R. A. Zanon; F. Yu; P. Musacchio; L. Lewald; M. Zollo; K. Krauskopf; D. Mrdović; P. Raunft; T. E. Maher; M. Cigler; C. Chang; K. Lang; F. D. Toste; A. I. Nesvizhskii; S. M. Hacker Profiling the Proteome-Wide Selectivity of Diverse Electrophiles. July 12, 2021. doi: DOI: **10.26434/chemrxiv-2021-w7rss-v2**.

18 M. Lim, T. D. Cong, L. M. Orr, E. S. Toriki, A. C. Kile, J. W. Papatzimas, E. Lee, Y. Lin and D. K. Nomura, DCAF16-Based Covalent Handle for the Rational Design of Monovalent Degraders, *ACS Cent. Sci.*, 2024, **10**(7), 1318–1331, DOI: **10.1021/acscentsci.4c00286**.

19 R. R. Shah, E. De Vita, P. S. Sathyamurthi, D. Conole, X. Zhang, E. Fellows, E. R. Dickinson, C. M. Fleites, M. A. Queisser, J. D. Harling and E. W. Tate, Structure-Guided Design and Optimization of Covalent VHL-Targeted Sulfonyl Fluoride PROTACs, *J. Med. Chem.*, 2024, **67**(6), 4641–4654, DOI: **10.1021/acs.jmedchem.3c02123**.

20 M. B. Cordon, K. M. Jacobsen, C. S. Nielsen, P. Hjerrild and T. B. Poulsen, Forward Chemical Genetic Screen for Oxygen-Dependent Cytotoxins Uncovers New Covalent Fragments That Target GPX4, *ChemBioChem*, 2022, **23**(1), e202100253, DOI: **10.1002/cbic.202100253**.

21 Q. Zheng, J. L. Woehl, S. Kitamura, D. Santos-Martins, C. J. Smedley, G. Li, S. Forli, J. E. Moses, D. W. Wolan and K. B. Sharpless, SuFEx-Enabled, Agnostic Discovery of Covalent Inhibitors of Human Neutrophil Elastase, *Proc. Natl. Acad. Sci. U.S.A.*, 2019, **116**(38), 18808–18814, DOI: **10.1073/pnas.1909972116**.

22 M. Gersch, J. Kreuzer and S. A. Sieber, Electrophilic Natural Products and Their Biological Targets, *Nat. Prod. Rep.*, 2012, **29**(6), 659, DOI: **10.1039/c2np20012k**.

23 P. Gehrtz and N. London, Electrophilic Natural Products as Drug Discovery Tools, *Trends Pharmacol. Sci.*, 2021, **42**(6), 434–447, DOI: **10.1016/j.tips.2021.03.008**.

24 G. J. Wørmer, N. L. Villadsen, P. Nørby and T. B. Poulsen, Concise Asymmetric Syntheses of Streptazone A and Abikoviromycin, *Angew. Chem., Int. Ed.*, 2021, **60**(19), 10521–10525, DOI: **10.1002/anie.202101439**.

25 H. Raistrick and G. Smith, Studies in the Biochemistry of Micro-Organisms, *Biochem. J.*, 1935, **29**(3), 606–611, DOI: **10.1042/bj0290606**.

26 Y. Honmura, S. Uesugi, H. Maeda, K. Tanaka, T. Nehira, K. Kimura, M. Okazaki and M. Hashimoto, Isolation, Absolute Structures, and Biological Properties of Cyclohelminthols I–IV from Helminthosporium Velutinum Yone96, *Tetrahedron*, 2016, **72**(10), 1400–1405, DOI: **10.1016/j.tet.2016.01.036**.

27 M. F. Elsebai, H. A. Ghabbour, N. Legrave, F. Fontaine-Vive and M. Mehiri, New Bioactive Chlorinated Cyclopentene Derivatives from the Marine-Derived Fungus Phoma Sp, *Med. Chem. Res.*, 2018, **27**(8), 1885–1892, DOI: **10.1007/s00044-018-2201-1**.

28 M. Zhao, D.-L. Guo, G.-H. Liu, X. Fu, Y.-C. Gu, L.-S. Ding and Y. Zhou, Antifungal Halogenated Cyclopentenones from the Endophytic Fungus *Saccharicola Bicolor* of *Bergenia Purpurascens* by the One Strain-Many Compounds Strategy, *J. Agric. Food Chem.*, 2020, **68**(1), 185–192, DOI: **10.1021/acs.jafc.9b06594**.

29 G. M. Strunz, A. S. Court, J. Komlossy and M. A. Stillwell, Structure of Cryptosporiopsin: A New Antibiotic Substance Produced by a Species of *Cryptosporiopsis*, *Can. J. Chem.*, 1969, **47**(11), 2087–2094, DOI: **10.1139/v69-335**.

30 V. Mierau, O. Sterner and T. Anke, Two New Biologically Active Cyclopentenones from Dasyscyphus Sp. A47-98, *J. Antibiot.*, 2004, **57**(5), 311–315, DOI: **10.7164/antibiotics.57.311**.

31 T. Matsumoto, T. Hosoya, H. Tomoda, M. Shiro and H. Shigemori, Palmaenones A and B, Two New Antimicrobial Chlorinated Cyclopentenones from Discomycete Lachnum Palmae, *Chem. Pharm. Bull.*, 2011, **59**(12), 1559–1561, DOI: **10.1248/cpb.59.1559**.

32 T. T. Curran, D. A. Hay, C. P. Koegel and J. C. Evans, The Preparation of Optically Active 2-Cyclopenten-l,4-Diol Derivatives from Furfuryl Alcohol, *Tetrahedron*, 1997, **53**, 1983–2004.

33 T. Schlama, K. Gabriel, V. Gouverneur and C. Mioskowski, Tetraethylammonium Trichloride: A Versatile Reagent for Chlorinations and Oxidations, *Angew. Chem., Int. Ed.*, 1997, **36**(21), 2342–2344, DOI: **10.1002/anie.199723421**.

34 K. C. Nicolaou, D. L. F. Gray, T. Montagnon and S. T. Harrison, Oxidation of Silyl Enol Ethers by Using IBX and IBX·N-Oxide Complexes: A Mild and Selective Reaction for the Synthesis of Enones, *Angew. Chem., Int. Ed.*, 2002, **41**(6), 996–1000, DOI: **10.1002/1521-3773(20020315)41:6<996::AID-ANIE996>3.0.CO;2-I**.

35 Y. Horiguchi, M. Komatsu and I. Kuwajima, Does Me3SiCl Activate Conjugate Addition of Copper Reagents as a Lewis Acid, *Tetrahedron Lett.*, 1989, **30**(50), 7087–7090, DOI: **10.1016/S0040-4039(01)93430-6**.

36 S. Matsuzawa, Y. Horiguchi, E. Nakamura and I. Kuwajima, Chlorosilane-Accelerated Conjugate Addition of Catalytic and Stoichiometric Organocopper Reagents, *Tetrahedron*, 1989, **45**(2), 349–362, DOI: **10.1016/0040-4020(89)80064-X**.

37 R. Shrestha, S. C. M. Dorn and D. J. Weix, Nickel-Catalyzed Reductive Conjugate Addition to Enones *via* Allylnickel Intermediates, *J. Am. Chem. Soc.*, 2013, **135**(2), 751–762, DOI: 10.1021/ja309176h.

38 G. Li, M. Obul, J. Zhao, G. Liu, W. Lu and H. A. Aisa, Novel Amides Modified Rupestonic Acid Derivatives as Anti-Influenza Virus Reagents, *Bioorg. Med. Chem. Lett.*, 2019, **29**(19), 126605, DOI: 10.1016/j.bmcl.2019.08.009.

39 P. A. Wender and D. A. Holt, Macroexpansion Methodology. 3. Eight-Step Synthesis of (-)-(3Z)-Cembrene A, *J. Am. Chem. Soc.*, 1985, **107**(25), 7771–7772, DOI: 10.1021/ja00311a096.

40 M.-A. Bray, S. Singh, H. Han, C. T. Davis, B. Borgeson, C. Hartland, M. Kost-Alimova, S. M. Gustafsdottir, C. C. Gibson and A. E. Carpenter, Cell Painting, a High-Content Image-Based Assay for Morphological Profiling Using Multiplexed Fluorescent Dyes, *Nat. Protoc.*, 2016, **11**(9), 1757–1774, DOI: 10.1038/nprot.2016.105.

41 E. B. Svenningsen and T. B. Poulsen, Establishing Cell Painting in a Smaller Chemical Biology Lab – A Report from the Frontier, *Bioorg. Med. Chem.*, 2019, **27**(12), 2609–2615, DOI: 10.1016/j.bmc.2019.03.052.

42 S. Lin, H. Liu, E. B. Svenningsen, M. Wollesen, K. M. Jacobsen, F. D. Andersen, J. Moyano-Villameriel, C. N. Pedersen, P. Nørby, T. Tørring and T. B. Poulsen, Expanding the Antibacterial Selectivity of Polyether Ionophore Antibiotics through Diversity-Focused Semisynthesis, *Nat. Chem.*, 2021, **13**(1), 47–55, DOI: 10.1038/s41557-020-00601-1.

43 J. L. Dahlin, B. K. Hua, B. E. Zucconi, S. D. Nelson, S. Singh, A. E. Carpenter, J. H. Shrimp, E. Lima-Fernandes, M. J. Wawer, L. P. W. Chung, A. Agrawal, M. O'Reilly, D. Barsyte-Lovejoy, M. Szewczyk, F. Li, P. Lak, M. Cuellar, P. A. Cole, J. L. Meier, T. Thomas, J. B. Baell, P. J. Brown, M. A. Walters, P. A. Clemons, S. L. Schreiber and B. K. Wagner, Reference Compounds for Characterizing Cellular Injury in High-Content Cellular Morphology Assays, *Nat. Commun.*, 2023, **14**(1), 1364, DOI: 10.1038/s41467-023-36829-x.

44 L. Laraia, G. Garivet, D. J. Foley, N. Kaiser, S. Müller, S. Zinken, T. Pinkert, J. Wilke, D. Corkery, A. Pahl, S. Sievers, P. Janning, C. Arenz, Y. Wu, R. Rodriguez and H. Waldmann, Image-Based Morphological Profiling Identifies a Lysosomotropic, Iron-Sequestering Autophagy Inhibitor, *Angew. Chem., Int. Ed.*, 2020, **59**(14), 5721–5729, DOI: 10.1002/anie.201913712.

45 S. Rezaei Adariani, D. Agne, S. Koska, A. Burhop, C. Seitz, J. Warmers, P. Janning, M. Metz, A. Pahl, S. Sievers, H. Waldmann and S. Ziegler, Detection of a Mitochondrial Fragmentation and Integrated Stress Response Using the Cell Painting Assay, *J. Med. Chem.*, 2024, **67**(15), 13252–13270, DOI: 10.1021/acs.jmedchem.4c01183.

46 J. E. Hutz, T. Nelson, H. Wu, G. McAllister, I. Moutsatsos, S. A. Jaeger, S. Bandyopadhyay, F. Nigsch, B. Cornett, J. L. Jenkins and D. W. Selinger, The Multidimensional Perturbation Value: A Single Metric to Measure Similarity and Activity of Treatments in High-Throughput Multidimensional Screens, *SLAS Discovery*, 2013, **18**(4), 367–377, DOI: 10.1177/1087057112469257.

47 M. M. Blewett, J. Xie, B. W. Zaro, K. M. Backus, A. Altman, J. R. Teijaro and B. F. Cravatt, Chemical Proteomic Map of Dimethyl Fumarate–Sensitive Cysteines in Primary Human T Cells, *Sci. Signaling*, 2016, **9**(445), rs10, DOI: 10.1126/scisignal.aaf7694.

48 K. K. Brown and M. B. Hampton, Biological Targets of Isothiocyanates, *Biochim. Biophys. Acta, Gen. Subj.*, 2011, **1810**(9), 888–894, DOI: 10.1016/j.bbagen.2011.06.004.

49 M. Tintore, A. Vidal-Jordana and J. Sastre-Garriga, Treatment of Multiple Sclerosis — Success from Bench to Bedside, *Nat. Rev. Neurol.*, 2019, **15**(1), 53–58, DOI: 10.1038/s41582-018-0082-z.

50 M. Ahuja, N. Ammal Kaidery, L. Yang, N. Calingasan, N. Smirnova, A. Gaisin, I. N. Gaisina, I. Gazaryan, D. M. Hushpulian, I. Kaddour-Djebbar, W. B. Bollag, J. C. Morgan, R. R. Ratan, A. A. Starkov, M. F. Beal and B. Thomas, Distinct Nrf2 Signaling Mechanisms of Fumaric Acid Esters and Their Role in Neuroprotection against 1-Methyl-4-Phenyl-1,2,3,6-Tetrahydropyridine-Induced Experimental Parkinson's-Like Disease, *J. Neurosci.*, 2016, **36**(23), 6332–6351, DOI: 10.1523/JNEUROSCI.0426-16.2016.

51 L. Casares, V. García, M. Garrido-Rodríguez, E. Millán, J. A. Collado, A. García-Martín, J. Peñarando, M. A. Calzado, L. De La Vega and E. Muñoz, Cannabidiol Induces Antioxidant Pathways in Keratinocytes by Targeting BACH1, *Redox Biol.*, 2020, **28**, 101321, DOI: 10.1016/j.redox.2019.101321.

52 N. Kurmasheva, A. Said, B. Wong, P. Kinderman, X. Han, A. H. F. Rahimic, A. Kress, M. E. Carter-Timofte, E. Holm, D. Van Der Horst, C. F. Kollmann, Z. Liu, C. Wang, H.-D. Hoang, E. Kovalenko, M. Chrysopoulou, K. S. Twayana, R. N. Ottosen, E. B. Svenningsen, F. Begnini, A. E. Kiib, F. E. H. Kromm, H. J. Weiss, D. Di Carlo, M. Muscolini, M. Higgins, M. Van Der Heijden, A. Bardoul, T. Tong, A. Ozsvar, W.-H. Hou, V. R. Schack, C. K. Holm, Y. Zheng, M. Ruzek, J. Kalucka, L. De La Vega, W. A. M. Elgaher, A. R. Korshoej, R. Lin, J. Hiscott, T. B. Poulsen, L. A. O'Neill, D. G. Roy, M. M. Rinschen, N. Van Montfoort, J.-S. Diallo, H. F. Farin, T. Alain and D. Olagnier, Octyl Itaconate Enhances VSVΔ51 Oncolytic Virotherapy by Multitarget Inhibition of Antiviral and Inflammatory Pathways, *Nat. Commun.*, 2024, **15**(1), 4096, DOI: 10.1038/s41467-024-48422-x.

53 S. W. Ryter, Heme Oxygenase-1: An Anti-Inflammatory Effector in Cardiovascular, Lung, and Related Metabolic Disorders, *Antioxidants*, 2022, **11**(3), 555, DOI: 10.3390/antiox11030555.

54 E. H. Krenske, R. C. Petter and K. N. Houk, Kinetics and Thermodynamics of Reversible Thiol Additions to Mono- and Diactivated Michael Acceptors: Implications for the Design of Drugs That Bind Covalently to Cysteines, *J. Org. Chem.*, 2016, **81**(23), 11726–11733, DOI: 10.1021/acs.joc.6b02188.

55 J. Yu, X. Yang, Y. Sun and Z. Yin, Highly Reactive and Tracelessly Cleavable Cysteine-Specific Modification of Proteins *via* 4-Substituted Cyclopentenone, *Angew. Chem., Int. Ed.*, 2018, **57**(36), 11598–11602, DOI: **10.1002/anie.201804801**.

56 P. Eckenberg, U. Groth, T. Huhn, N. Richter and C. Schmeck, A Useful Application of Benzyl Trichloroacetimidate for the Benzylation of Alcohols, *Tetrahedron*, 1993, **49**(8), 1619–1624, DOI: **10.1016/S0040-4020(01)80349-5**.

57 H.-Y. Chang, A. T. Kong, F. Da Veiga Leprevost, D. M. Avtonomov, S. E. Haynes and A. I. Nesvizhskii, Crystal-C: A Computational Tool for Refinement of Open Search Results, *J. Proteome Res.*, 2020, **19**(6), 2511–2515, DOI: **10.1021/acs.jproteome.0c00119**.

58 G. C. Teo, D. A. Polasky, F. Yu and A. I. Nesvizhskii, Fast Deisotoping Algorithm and Its Implementation in the MSFragger Search Engine, *J. Proteome Res.*, 2021, **20**(1), 498–505, DOI: **10.1021/acs.jproteome.0c00544**.

59 F. Yu, G. C. Teo, A. T. Kong, S. E. Haynes, D. M. Avtonomov, D. J. Geiszler and A. I. Nesvizhskii, Identification of Modified Peptides Using Localization-Aware Open Search, *Nat. Commun.*, 2020, **11**(1), 4065, DOI: **10.1038/s41467-020-17921-y**.

60 A. T. Kong, F. V. Leprevost, D. M. Avtonomov, D. Mellacheruvu and A. I. Nesvizhskii, MSFragger: Ultrafast and Comprehensive Peptide Identification in Mass Spectrometry–Based Proteomics, *Nat. Methods*, 2017, **14**(5), 513–520, DOI: **10.1038/nmeth.4256**.

61 F. Da Veiga Leprevost, S. E. Haynes, D. M. Avtonomov, H.-Y. Chang, A. K. Shanmugam, D. Mellacheruvu, A. T. Kong and A. I. Nesvizhskii, Philosopher: A Versatile Toolkit for Shotgun Proteomics Data Analysis, *Nat. Methods*, 2020, **17**(9), 869–870, DOI: **10.1038/s41592-020-0912-y**.

62 D. J. Geiszler, A. T. Kong, D. M. Avtonomov, F. Yu, F. D. V. Leprevost and A. I. Nesvizhskii, PTM-Shepherd: Analysis and Summarization of Post-Translational and Chemical Modifications From Open Search Results, *Mol. Cell. Proteomics*, 2021, **20**, 100018, DOI: **10.1074/mcp.TIR120.002216**.

63 E. Resnick, A. Bradley, J. Gan, A. Douangamath, T. Krojer, R. Sethi, P. P. Geurink, A. Aimon, G. Amitai, D. Bellini, J. Bennett, M. Fairhead, O. Fedorov, R. Gabizon, J. Gan, J. Guo, A. Plotnikov, N. Reznik, G. F. Ruda, L. Díaz-Sáez, V. M. Straub, T. Szommer, S. Velupillai, D. Zaidman, Y. Zhang, A. R. Coker, C. G. Dowson, H. M. Barr, C. Wang, K. V. M. Huber, P. E. Brennan, H. Ovaa, F. Von Delft and N. London, Rapid Covalent-Probe Discovery by Electrophile-Fragment Screening, *J. Am. Chem. Soc.*, 2019, **141**(22), 8951–8968, DOI: **10.1021/jacs.9b02822**.

64 C. Dubiella, B. J. Pinch, K. Koikawa, D. Zaidman, E. Poon, T. D. Manz, B. Nabet, S. He, E. Resnick, A. Rogel, E. M. Langer, C. J. Daniel, H.-S. Seo, Y. Chen, G. Adelmant, S. Sharifzadeh, S. B. Ficarro, Y. Jamin, B. Martins Da Costa, M. W. Zimmerman, X. Lian, S. Kibe, S. Kozono, Z. M. Doctor, C. M. Browne, A. Yang, L. Stoler-Barak, R. B. Shah, N. E. Vangos, E. A. Geffken, R. Oren, E. Koide, S. Sidi, Z. Shulman, C. Wang, J. A. Marto, S. Dhe-Paganon, T. Look, X. Z. Zhou, K. P. Lu, R. C. Sears, L. Chesler, N. S. Gray and N. London, Sulfopin Is a Covalent Inhibitor of Pin1 That Blocks Myc-Driven Tumors in Vivo, *Nat. Chem. Biol.*, 2021, **17**(9), 954–963, DOI: **10.1038/s41589-021-00786-7**.